In Vivo Validation of Magnetic Resonance Blood Volume Flow Measurements with Limited Spatial Resolution in Small Vessels

Mark B. M. Hofman, Frans C. Visser, Albert C. van Rossum, Ger Q. M. Vink, Michiel Sprenger, Nico Westerhof

The accuracy of magnetic resonance phase contrast volume flow measurements in small blood vessels is expected to be smaller than in large vessels, because of partial volume effects at the vessel boundary. Accuracy was validated in the dog femoral artery, diameter 3.5 ± 0.7 mm, using an ultrasonic transit-time flowmeter (TT). The number of pixels per vessel diameter (N_D) ranged from 1.6 to 4.8. The vessel cross-section was determined using a threshold in the magnitude image. Between the two methods the correlation coefficient was 0.95 (range 10–200 ml/min). The proportional difference (PD), $(Q_{TT} - Q_{MR})/½(Q_{TT} + Q_{MR})$, was 0.8%, showing no systematic difference between the methods. The PDs standard deviation was 27%, and 19% for flow rates above 30 ml/min. Only a significant decrease of the PDs variance was found at the highest N_D values, suggesting other sources of error than partial volume effects. It is concluded that with an N_D value of about 3, accurate blood volume flow rates can be determined.

Key words: volume flow; MRI; accuracy; flow quantification.

INTRODUCTION

Magnetic resonance (MR) imaging offers the possibility of determining blood flow based on flow-induced phase effects (1, 2). Using the phase difference of two data sets with different first gradient moments, acquired in an interleaved fashion, a one-directional velocity pixel map can be calculated (3, 4). If the image plane is positioned perpendicularly to the vessel, and the velocity encoding direction is along the vessel direction, volume flow can be obtained by integration of the velocity over the vessel cross-section. When flow is pulsatile, as is the case in arteries, the measurements are typically performed in a cine mode, gated to the cardiac cycle. By a second integration over time, the mean volume flow can be determined. This MR phase contrast flow measurement technique is clinically used to determine volume flow in large- to medium-sized vessels, with diameters from 6 to 25 mm (5, 6).

MRM 33:778–784 (1995)

From the Departments of Physiology (M.B.M.H., N.W.), Clinical Physics & Engineering (M.B.M.H., M.S.), Cardiology (F.C.V., A.C.v.R.), Clinical Animal Experiments (G.Q.M.V.), ICaR-VU, ICIN, Free University, Amsterdam, The Netherlands.

Address correspondence to: Mark Hofman, Ph.D., Department of Clinical Physics & Engineering, Free University Hospital, De Boelelaan 1117, 1081 HV Amsterdam, The Netherlands.

Received October 10, 1994; revised January 25, 1995; accepted February 20, 1995.

0740-3194/95 $3.00

In vitro experiments have demonstrated that the inaccuracies of both velocities and volume flows in large vessels are about 5–10%, both under continuous and pulsatile flow conditions (7–10). Also, several *in vivo* validation studies of volume flow in large vessels are reported in the literature (11–16). Maier *et al.* compared MR flow with Doppler ultrasound in the human abdominal aorta. They showed a standard error of estimation (SEE) in the flow volume per heart beat of 1.7 ml over a flow range from 10 to 25 ml (11). A comparison of cardiac stroke volume determined by MR flow measurements in the human aorta and by an indicator dilution technique gave a proportional difference (PD) of both methods of 1.5 ± 8% (12). Validation was also performed by comparison of left ventricular stroke volume determined with velocity measurements in the ascending aorta and with volume changes of the left ventricle. A mean PD between the two methods of 1 ± 10% in the range from 50 to 100 ml (13), and a SEE of 3.3 ml in a studied range from 60 to 100 ml (14), were reported.

All these validations were performed in large vessels or tubes. A decrease of the vessel diameter relative to the spatial resolution will affect the accuracy of the volume flow measurement. Velocity values appeared to be correct in the center of small vessels, as shown *in vitro* (8) and *in vivo* (17). However, the relative amount of pixels at the vessel boundary increases as the vessel diameter gets smaller. This leads to a larger contribution of the partial volume effect at the vessel boundary (5, 18, 19). *In vitro* studies and simulations showed that these effects may cause large systematic errors in the volume flow determination (19, 20).

In vivo validation of the volume flow in small vessels with a limited resolution has not been described in the literature so far. The only possible noninvasive method to compare with, is pulsed Doppler combined with 2D ultrasound imaging. However, the absolute accuracy of Doppler ultrasound is variable (21), and the sample resolution to determine volume flow in these small vessels is limited (22). Therefore, studies are to be performed, using an invasive method to determine volume flow for comparison.

The purpose of this study was to achieve an *in vivo* validation of magnetic resonance volume flow in small vessels with a diameter around 3 mm with a limited in-plane resolution. Volume flow was determined by MR with a cine phase contrast 2D velocity measurement with the image plane perpendicular to the vessel. For comparison an ultrasonic transit-time volume flow probe was placed around the vessel (23).

MATERIALS AND METHODS

Animal Preparation

Volume flow measurements were performed in the femoral artery of the dog (diameter 3.5 ± 0.7 mm). The protocol was approved by the ethical committee on animal experiments of the Free University. Eleven mongrel dogs weighing 24 ± 4 kg were used. The animals were anesthetized with a combination of ketamine hydrochloride (15 mg/kg, intramuscularly) and xylazine hydrochloride (1.2 mg/kg, intramuscularly) without artificial ventilation. The upper femoral artery was isolated over a length of 3 cm, and the perivascular transit-time flow probe was positioned around the vessel (see below). The space between the vessel and the probe was filled with an acoustic gel to obtain good ultrasound transmission. If any side vessel was observed, it was ligated. ECG electrodes were adhered to the chest to perform cardiac triggering of the MR acquisition. The animals were placed in supine position inside the MR scanner bore.

Equipment

The MR measurements were performed on a super-conducting 1.5 Tesla whole body MR scanner (Magnetom 63SP, Siemens Medical Systems, Erlangen, Germany). To optimize the signal-to-noise ratio, a standard circular RF receiver coil (diameter of 10 cm) was positioned above the vessel of interest.

For comparison with MR flow an ultrasonic transit-time flowmeter (Transonic Systems Inc., Ithaca, NY) with a perivascular probe (6RB250) was used (23, 24). These flow probes operate within the strong magnetic field of MR scanners (25). To limit MR image distortion by the probe, its metallic parts were made of brass only. The area of signal loss in the image extended less than 0.5 cm from the probe, as observed on gradient echo images with acquisition parameters identical to the parameters used in the flow measurements.

MR Measurements

To position the image plane of the flow measurement, first a 3D MR angiogram of the femoral artery was obtained. A 2D sequential time of flight angiographic technique (resolution 0.78 × 1.25 × 4 mm^3) was used (26, 27). The image plane of the flow acquisition was set perpendicularly to the vessel, 2 cm downstream from the ultrasonic probe center. On the angiogram it was verified that no side branches originated between the probe and MR image plane. Because of RF interference between the ultrasonic flowmeter and the MR machine (28), an ultrasonic flow measurement was obtained just before and just after the MR flow acquisition, but not during the MR acquisition.

For the MR flow measurement, the phase contrast method as described by Nayler *et al.* was used (4). An ECG triggered cine gradient echo pulse sequence with a repetition time of 17.5 ms and an echo-time of 6 ms was used. A velocity-compensated and a velocity-encoded sequence were interleaved within one cardiac cycle, resulting in a time resolution of 35 ms. The acquisitions were performed with a matrix of 256 × 256, a field of view of 250 × 250 mm^2, and a slice thickness of 6 mm, resulting in a voxel size of 0.98 × 0.98 × 6 mm^3. The scan duration was 4.3 min for a typical heart rate of 120 beats per min. The acquisition time after each trigger was 20% longer than the RR interval, to cover the whole cardiac cycle. The velocity sensitivity, defined by the velocity inducing a phase shift of π radians, was set at 40, 80, or 160 cm/s, with the minimum value just above the maximum velocity inside the vessel.

To obtain a range of volume flow measurements within one animal, the flow was increased by rapid administration of a plasma expander (gelofusine, 500 ml, intravenously, in 5 min) or by continuous infusion of epinephrine (0.1 to 0.4 mg/h, intravenously). To obtain a stable volume flow, we waited 5 to 10 min before each MR measurement. In all animals together, 34 measurements were performed perpendicularly to the vessel with a 1 × 1 mm^2 in-plane resolution. In eight animals, 11 additional flow measurements were acquired with a lower in-plane resolution of 1.95 × 1.95 mm^2.

Data Analysis

The data were processed off-line on a work-station (Sun Microsystems, Mountain View, CA). Only the time-averaged volume flow was considered, and not the phasic flow pattern. The time-averaged volume flow was calculated by integration of the velocities over the vessel cross-section and the cardiac cycle. Thus, to obtain volume flow, vessel boundaries need to be accurately determined. The vessel boundaries were determined semi-automatically by a seed growing algorithm on the velocity-compensated magnitude image of each time frame. First, a region of interest (ROI) was placed in the surrounding muscle tissue. Then, a pixel seed was positioned at the vessel center. The vessel boundary was generated by a growing algorithm with a magnitude lower border (threshold value) set at 50% of the difference between the magnitude signal of the surrounding tissue and the vessel center (18). In some cases, it was necessary to prevent the algorithm from growing into the neighboring femoral vein cross-sectional area. To illustrate the effect of this threshold value, it was changed over the range from 35–75% in one typical case. The velocity values were corrected for a velocity offset, caused by eddy current-induced phase shifts (5). This offset was determined in each velocity image by two extra ROIs in stationary muscle tissue, close to the vessel. These ROIs were positioned symmetrically with respect to the vessel, taking spatial gradients in the offset into account. Figure 1 shows an example of a magnitude image of a flow acquisition with the different ROIs.

To determine whether pixel interpolation would reduce the partial volume effect, the same data were also analyzed after pixel interpolation to a four × smaller pixel size, obtained by zero padding in *k*-space. A third analysis was performed on the data after an interpolation of only the magnitude images. This was based on the hypothesis that interpolation in the magnitude image would give a more accurate cross-section, while velocity values are correct because of the larger magnitude in the vessel relative to the surrounding tissue.

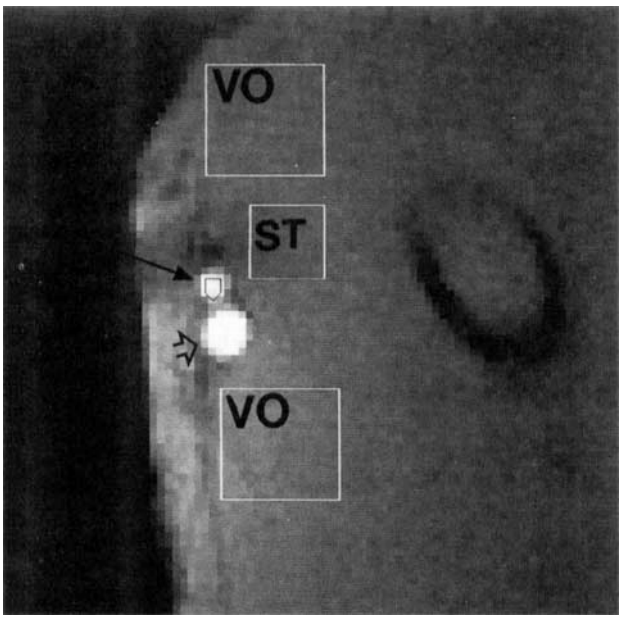

FIG. 1. A magnitude image of a flow acquisition, perpendicular to the dog femoral artery (solid arrow) and its adjacent femoral vein (open arrow). The different regions of interest are shown: the vessel boundary in the femoral artery (drawn at the center points of the border pixels of the ROI), the region to determine the signal intensity of surrounding tissue (ST), and in the two regions for the velocity offset correction (VO).

The vessel diameters (D) were determined from the cross-sectional area (A) on magnitude images with the growing algorithm, assuming $A = D^2\pi/4$. As a measure of intravoxel averaging, the number of pixels per vessel diameter (N_D) was calculated.

Statistical Analysis

The volume flow data of the two methods were compared with linear regression analysis, with the ultrasonic flow method as a standard of reference, resulting in a slope, an intercept, and a SEE. Also the correlation coefficient (r) was determined. A better method to assess agreement between two methods, with both their inaccuracy, is to consider the mean difference in volume flow (Q) between the two methods and its standard deviation (29). As most errors in both methods are relative errors, the PD was used, calculated as $(Q_{TT} - Q_{MR})/\frac{1}{2}(Q_{TT} + Q_{MR}) \times 100\%$. An analysis of variance (ANOVA) was performed to determine possible differences in PD between animals. The intraclass correlation was determined. The mean PD and its standard deviation (SD) over all experiments were determined in two ways, using all individual data points and using only the averaged value of each animal, whereby the second one is presented between parentheses. The first way optimally uses all data points; however, it assumes that different data points obtained within the same animal are independent of each other concerning all sources of error. The second way does not use this assumption. To determine the effect of the N_D value, the mean PD and its variance were calculated at four different ranges of N_D: 1.5–2.5, 2.5–3.5, 3.5–4.5, and 4.5–5.5. All mean PD were tested for a significant difference from zero, using the Student t test. Differences in variances were tested using the F value. Differences were considered significantly at $P < 0.05$.

RESULTS

The RR interval was in the range from 365 to 908 ms, with a mean ± SD of 525 ± 108 ms, resulting in 10–26 time frames per cardiac cycle. The internal vessel diameter was 3.5 ± 0.7 mm (range 1.6–4.7 mm). The volume flow was constant during the MR acquisition, with a mean PD of the ultrasonic volume flow measurements before and after of the MR acquisition of −0.9 ± 7%.

1-mm Spatial Resolution

For the 1 × 1 mm² resolution, the regression analysis revealed a high correlation coefficient of 0.95 between the volume flows determined by ultrasonic transit time (TT) and by MR, as shown in Fig. 2a (Q_{MR} = 0.96 (±0.05) × Q_{TT} + 1 (±4) with SEE = 14 ml/min). Figure 3a shows the PD as a function of the averaged volume flow of MR and ultrasound. ANOVA showed significant differences, with an intraclass correlation of 0.50, indicating systematic differences in PD between animals. The mean PD was 0.8 ± 27% (P = NS) (6 ± 25%), with a confidence interval of [−8.6–10.2%] ([−11–23%]). (The values between parentheses were calculated considering only the averaged PD of each animal.) For volume flows above 30 ml/min (n = 18), the mean PD was 2 ± 19% (P = NS) (−3.5 ± 22%). For volume flows below this value (n = 16), the PD was 3.5 ± 34% (P = NS) (0.9 ± 32%). The variance in the low flow range was significantly larger than for the high flow range, whereas the difference in mean PD was not significant.

Pixel Interpolation

After pixel interpolation of the 1 × 1 mm² in-plane resolution measurements, the resulting mean PD was 5.4 ± 27% (P = NS) (8.7 ± 24%). If only the magnitude images were interpolated, the mean PD was 8.4 ± 32% (P = NS) (13 ± 26%). Both the mean PD and the variances were not significantly different from the data obtained without interpolation.

2-mm Spatial Resolution

For the 11 measurements with the 2 × 2 mm² in-plane resolution, the linear regression equation over a range from 25 to 150 ml/min was $Q_{MR} = 0.78$ (±0.09) × Q_{TT} + 15 (±7) with $r = 0.94$ and SEE = 12 ml/min (see Fig. 2b). ANOVA did not show significant differences between the animals, and an intraclass correlation of 0.66 was found. The mean PD was −6 ± 33% (P = NS) (−8 ± 34%) with a confidence interval of [−28–36%] ([−20–35%]), which was not significantly different from the 1 × 1 mm² measurements. Also, no significant effect of interpolation was found, and the variance was also significantly lower for volume flows above 30 ml/min.

None of the conclusions depended on the way of calculation of the mean PD and its standard deviation, that

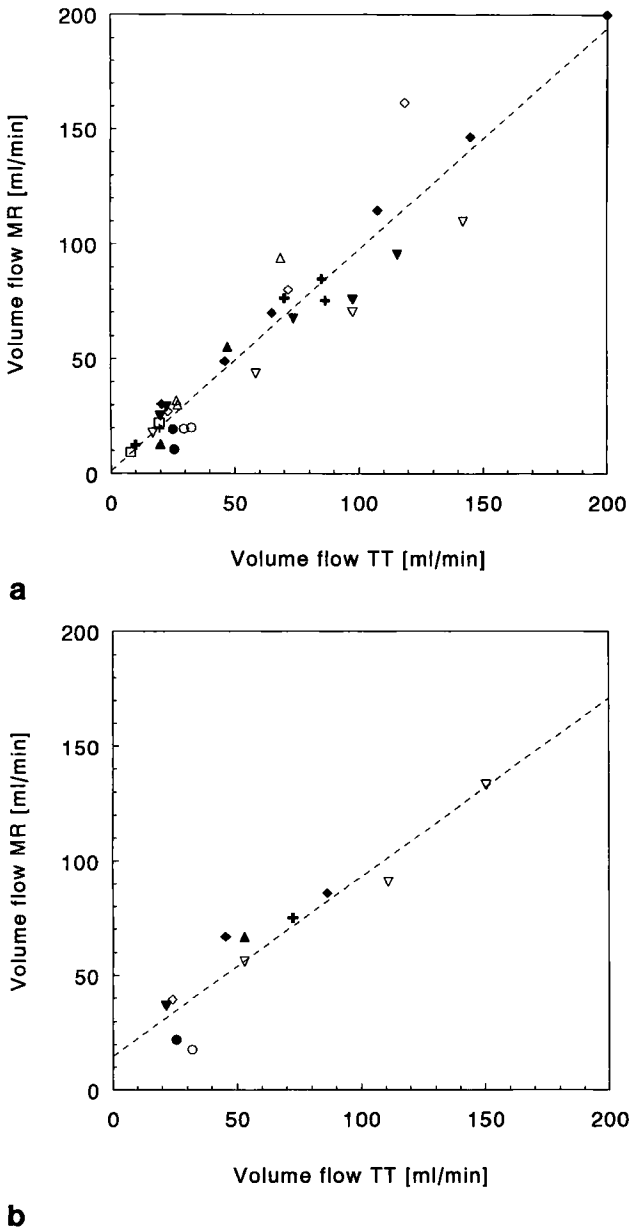

FIG. 2. The volume flow (Q) determined by magnetic resonance (MR) versus the volume flow determined by ultrasonic transit-time (TT) for the measurements with a 1 × 1 (a) and 2 × 2 (b) mm^2 in-plane resolution. The plotted line is obtained by linear regression (a: Q_{MR} = 0.96 (±0.05) × Q_{TT} + 1 (±4) with r = 0.95 and SEE = 14 ml/min; b: Q_{MR} = 0.78 (±0.09) × Q_{TT} + 15 (±7) with r = 0.94 and SEE = 12 ml/min). The different symbols represent values of different animal experiments.

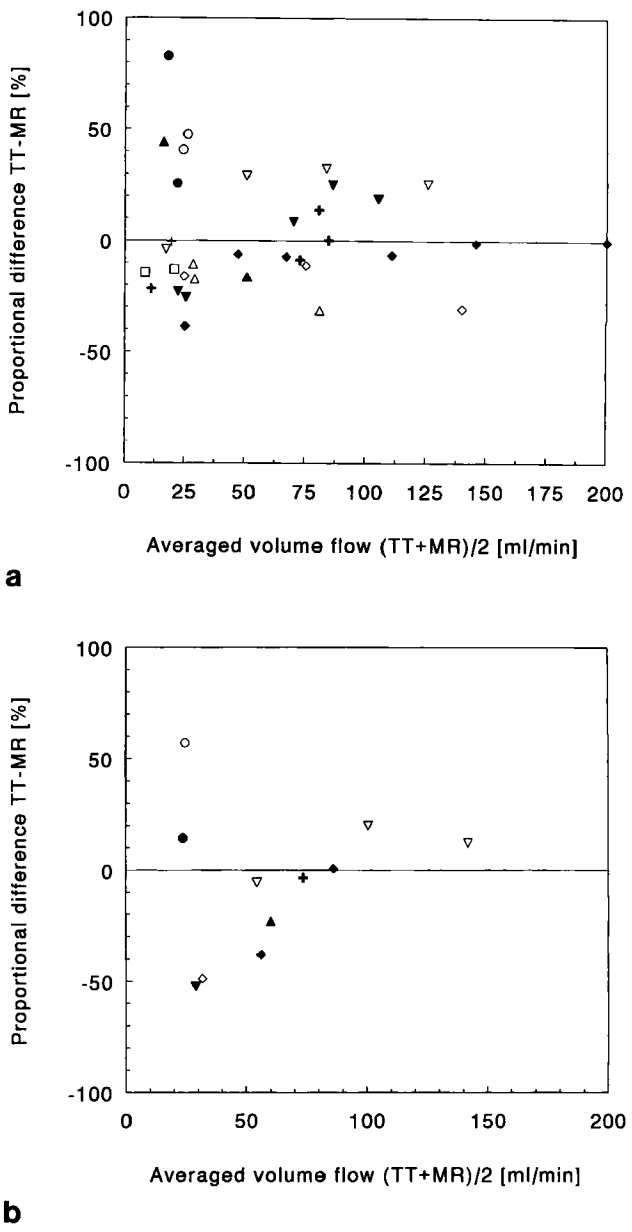

FIG. 3. The PD between the ultrasonic transit-time (TT) and the MR determined volume flows, versus their averaged value for the 1 × 1 (a) and 2 × 2 (b) mm^2 in-plane resolution. The experimental data points are the same as those in Fig. 2.

is from all individual data points or from the averaged values per animal.

The ratio of the signal magnitude of vessel to surrounding tissue averaged over the cardiac cycle, and all the 36 1 × 1 mm^2 resolution experiments was 3.4 ± 0.6. The standard deviation of this ratio caused by variations over the cardiac cycle was only 0.4. The vessel boundary was set at the isointensity between intraluminal signal and surrounding signal, at the threshold of 50%. Figure 4 illustrates the effect of a change of this threshold on both the volume flow and the cross-sectional area for one experiment. A different threshold value will result in significantly different determined volume flow.

Effect of N_D

Figure 5 shows the PD of volume flow versus the number of N_D for both in-plane resolutions. In this graph, the data points with a volume flow above or below the 30 ml/min have a different symbol. No mean PD significantly different from zero was found at the different N_D values. There was some decrease of the variance of the PD at larger N_D values. This was only significantly around an N_D of 5. However, all the data points at this N_D were obtained within one single animal.

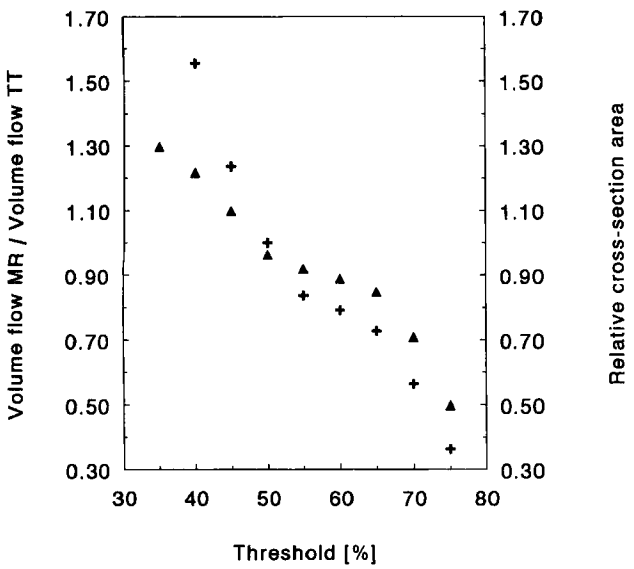

FIG. 4. Illustration of the effect of the threshold value in the vessel boundary determination on both the volume flow (▲ with the left *y* axis), relative to the volume flow determined by ultrasonic transit-time (TT), and the relative vessel cross-section (+ with the right *y* axis) determined by the growing algorithm. The data are from an acquisition with a 1 × 1 mm^2 in-plane resolution in the vessel shown in Fig. 1 (cross-section of 11 mm^2, N_D (see text) of 3.8).

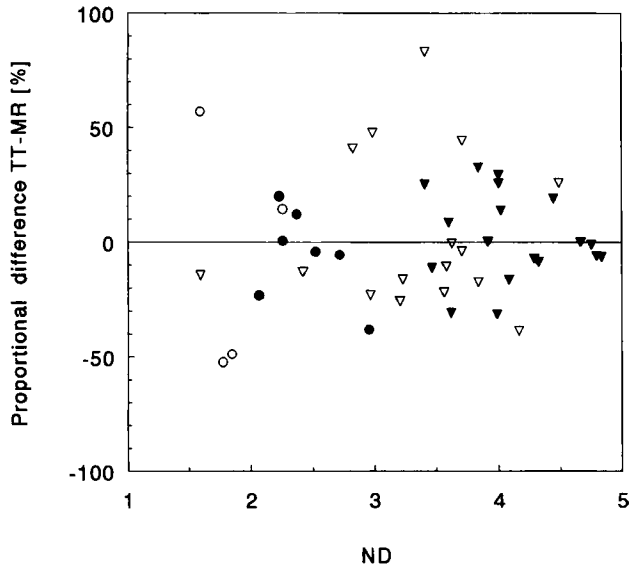

FIG. 5. Dependency of the PD in volume flow determined by ultrasonic transit-time (TT) and MR on the number of pixels per vessel diameter (N_D). Both the data with a 1 × 1 (▼ ▽) and 2 × 2 (● ○) mm^2 in-plane acquisition resolution are shown. The open and solid symbols represent data points with a volume flow below and above 30 ml/min, respectively.

DISCUSSION

The purpose of this study was to validate magnetic resonance phase contrast volume flow measurements in small vessels with a limited image resolution through comparison with an ultrasonic transit-time flowmeter. A good correlation of 0.95 between the two methods was found over a range from 10 to 200 ml/min. The mean PD between the two methods was 0.8% (P = NS), showing no significant systematic difference between the two methods. The standard deviation in the PD was 27%, with a significantly higher value for the volume flow range below 30 ml/min. After pixel interpolation the standard deviation of the PD did not decrease significantly. Also, a decrease in image resolution to 2 × 2 mm^2 did not alter these results significantly.

Partial Volume Effect

At the vessel boundary voxels contain both signal from vessel lumen and from surrounding tissue, resulting in a partial volume effect. The velocity value acquired with MR is determined from the phase of the averaged complex MR signal over the voxel. This MR-determined velocity in the boundary voxel is not per definition identical to the averaged velocity over the voxel volume. There are two effects that can cause a difference between the averaged velocity and the velocity determined from the averaged MR signal. First, if there are large velocity-induced differences in phase over the voxel, the phase of the averaged signal will differ from the averaged phase. This can be limited as suggested by Tarnawski *et al.* by reducing the velocity-induced phase shifts to less than 0.5π (30). Second, if the MR signal magnitude in the vessel is larger than that of the surrounding tissue, the phase of the vessel compartment within the voxel will have a larger contribution to the phase of the averaged signal, resulting in an overestimation of the MR determined velocity and volume flow (5).

For MR flow measurements usually a gradient echo imaging technique with a short repetition time is used. This causes a strong saturation of stationary tissue. However, for flowing blood the MR signal is less saturated, resulting in a larger MR signal within the vessel. This second effect of partial volume averaging, caused by a difference in signal magnitude between blood and stationary tissue, is the main source of error with respect to the velocity value of boundary voxels.

To determine the volume flow, the velocity value is integrated over the voxels within the vessel, i.e., the ROI. If the velocity value of each voxel is the correct averaged velocity over the voxel volume, then the ROI can be made larger than the vessel cross-section itself, and errors in determining the ROI extent would be avoided because the velocity outside the vessel is zero (30). However, because of the difference in signal magnitude between vessel and surrounding tissue, this approach would result in an overestimation of the volume flow. This overestimation can be limited by choosing an ROI based on a threshold in the signal magnitude (18, 19), as shown in Fig. 4. A threshold of 50%, the isointensity between intraluminal signal and surrounding signal is theoretically the correct value for plug flow. *In vitro*, it was shown to be also correct for laminar flow (19).

N_D Value

The influence of the partial volume effect on the accuracy of the volume flow depends on the ratio of the number of pixels in the cross-sectional area to the number of pixels at the vessel boundary. This ratio depends

linearly on the number of pixels per vessel diameter (N_D). This parameter is equal to the $D/\Delta x$ ratio as used by Wolf *et al.* (20). If this value is small, the partial volume effect will limit the accuracy of the volume flow determination.

In the present study, the N_D varied over a range from 1.6 to 4.8. No systematic PD between the two methods of volume flow determination was found over the whole range of N_D values. There was only a weak trend of the variance in the PD to the N_D. This may be due to the limited number of data points to determine an accurate variance, and to the large variance by other sources of error. The data suggest that the partial volume effect is not the main source of error.

General Accuracy of the Methods

The variance found in PD between both methods is caused by errors in the MR measurement and the ultrasound transit-time flow determination. The accuracy of the MR system was tested *in vitro* with a method described previously (8). In a tube (diameter 10 mm), the PD of the volume flow determined with MR and a float flowmeter was $-0.13 \pm 2.5\%$. In the *in vivo* measurements, the signal-to-noise ratio within the vessels was approximately 70, resulting in a statistical error in the volume flow of 3% or less (31). The misalignment of flow and velocity-encoding direction in our study was small, less than 10°, which results in errors less than 10% (19, 20). Thus, these errors do not explain the variation found.

The ultrasonic probe had a specified absolute inaccuracy of 15%, with a maximum offset of 10 ml/min, at a vessel diameter range from 3 to 6 mm. In one animal a vessel of less than 3 mm internal diameter was present. Because it is an absolute error, the variation in offset of the ultrasonic method can explain the large standard deviation found at volume flow values below 30 ml/min. Furthermore, *in vitro* testing of the probe, using a tube diameter of 4.7 mm, showed only small variations. However, using a tube with a diameter of 3 mm yielded variations in absolute inaccuracy up to 30%.

Another possible explanation of the large standard deviation of the PD is the effect of the statistical variation in MR signal magnitude on the vessel boundary growing. From Fig. 4 and the signal-to-noise ratio of the images, it was deduced that at an N_D of 4 this error in volume flow is below 10%. Also, the vessel boundary growing algorithm assumes a constant surrounding signal magnitude. This assumption was not always true. Sometimes, a small darker region adjacent to the vessel was observed, whereas the surrounding tissue magnitude was determined by muscle tissue. This variation in signal intensity around the vessel leads to an incorrect region of interest determination when using a fixed threshold. This may also partly explain the observed variation in the volume flow.

Thus, the large variance found in the comparison in the measurement is not determined by a single factor. The mentioned sources of error are independent to each other. Therefore, the net error can be calculated by a squared summation. This resulted in a net error comparable with the found variance, with a similar error contribution by the MR and the ultrasonic methods (each 15%). Only in case of vessels with a diameter of 3 mm or less, the net error is expected to be mainly determined by the ultrasonic method.

Other Studies

A number of other studies have been published addressing the same subject. Wolf *et al.* performed a simulation study with *in vitro* validation (20). They used an ROI larger than the cross-sectional area, causing a systematic overestimation of the volume flow in the order of 20% (N_D of 4) to 60% (N_D of 2). Tang *et al.* also described simulations and *in vitro* experiments (19). Using a large ROI and without a threshold, they found a 15–50% overestimation in volume flow. With a threshold of 50%, they found relative errors between the −15% and +20% at an N_D in the range from 2 to 5. From the small number of data of an *in vivo* validation in the aorta of the dog presented by Sebok *et al.*, we estimated a PD of $22 \pm 44\%$ (32). The variation we found is in the same order of magnitude as that reported by Wendt *et al.* (17). They performed an *in vivo* comparison of peak velocities in vessels with 2 to 4 pixels within the vessel cross-sectional area. In a recent study of Debatin *et al.*, the MR flow volume measurement in the renal artery was compared *in vivo* with para-aminohippurate clearance (15). A mean PD of $2.8 \pm 7\%$ was found. The averaged N_D value was 5.5, somewhat larger than in this study. They used an absolute threshold of 30%, in contrast to the relative threshold that we used. Theoretically, the use of a threshold relative to the surrounding tissue leads to more accurate results.

In Conclusion

The volume flow measurements, determined by phase contrast MR velocity measurements in small vessels (diameter 3 mm) with a limited spatial resolution compared with ultrasonic transit-time method, demonstrated a good correlation. However, the standard deviation of the difference between the two methods is large, even when partial volume effects are partly corrected with thresholding of the vessel cross-section relative to the signal magnitude.

ACKNOWLEDGMENTS

The authors thank B. van der Water for assistance in the animal handling, and F. Hoogenraad for his support in programming the postprocessing.

REFERENCES

1. T. P. Grover, J. R. Singer, NMR spin-echo flow measurement. *J. Appl. Phys.* **42**, 938–940 (1971).
2. P. R. Moran, A flow velocity zeugmatographic interlace for NMR imaging in humans. *Magn. Reson. Imaging* **1**, 197–203 (1982).
3. P. van Dijk, Direct cardiac NMR imaging of heart wall and blood flow velocity. *J. Comput. Assist. Tomogr.* **8**, 429–436 (1984).
4. G. L. Nayler, D. N. Firmin, D. B. Longmore, Blood flow

imaging by cine magnetic resonance. *J. Comput. Assist. Tomogr.* **10,** 715–722 (1986).
5. N. J. Pelc, R. J. Herfkens, A. Shimakawa, D. R. Enzmannn, Phase contrast cine magnetic resonance imaging. *Magn. Reson. Q.* **7,** 229–254 (1991).
6. R. H. Mohiaddin, D. B. Longmore, Functional aspects of cardiovascular nuclear magnetic resonance imaging Techniques and application. *Circulation* **88,** 264–281 (1993).
7. M. Kouwenhoven, M. B. M. Hofman, M. Sprenger, Accuracy of quantitative MR flow, measurement of pulsatile flow in a phantom, *in* "Proc., SMRM, 10th Annual Meeting, 1991," p. 807.
8. M. Kouwenhoven, M. B. M. Hofman, A. C. van Rossum, M. Sprenger, Validation and accuracy of quantitative MR flow measurement by means of a flow phantom, *in* "Proc., SMRM, 9th Annual Meeting, 1990," p. 472.
9. D. N. Ku, C. L. Biancheri, R. I. Pettigrew, J. W. Peifer, C. P. Markou, H. Engels, Evaluation of magnetic resonance velocimetry for steady flow. *J. Biomech. Eng.* **112,** 464–472 (1990).
10. P. J. Kilner, D. N. Firmin, R. S. Rees, J. Martinez, D. J. Pennell, R. H. Mohiaddin, S. R. Underwood, D. B. Longmore, Valve and great vessel stenosis: assessment with MR jet velocity mapping. *Radiology* **178,** 229–235 (1991).
11. S. E. Maier, D. Meier, P. Boesiger, U. T. Moser, A. Vieli, Human abdominal aorta: comparative measurements of blood flow with MR imaging and multigated Doppler US. *Radiology* **171,** 487–492 (1989).
12. J. Mogelvang, K. Lindvig, F. Stahlberg, C. Thompsen, M. Stubgaard, O. Hendriksen, Evaluation of in vivo blood flow by MRI at 1 T, *in* "Proc., SMRM, 8th Annual Meeting, 1989," p. 201.
13. A. C. van Rossum, M. Sprenger, F. C. Visser, K. H. Peels, J. Valk, J. P. Roos, An in vivo validation of quantitative blood flow imaging in arteries and veins using magnetic resonance phase-shift techniques. *Eur. Heart J.* **12,** 117–126 (1991).
14. D. N. Firmin, G. L. Nayler, R. H. Klipstein, S. R. Underwood, R. S. Rees, D. B. Longmore, In vivo validation of MR velocity imaging. *J. Comput. Assist. Tomogr.* **11,** 751–756 (1987).
15. J. F. Debatin, R. H. Ting, H. Wegmüller, F. G. Sommer, J. O. Fredrickson, T. J. Brosnan, B. S. Bowman, B. D. Myers, R. J. Herfkens, N. J. Pelc, Renal artery blood flow: quantification with phase contrast MR imaging with and without breath holding. *Radiology* **190,** 371–378 (1994).
16. R. I. Pettigrew, W. Dannels, J. R. Galloway, T. Pearson, W. Millikan, J. M. Henderson, J. Peterson, M. E. Bernardino, Quantitative phase-flow MR imaging in dogs by using standard sequences: comparison with in vivo flow-meter measurements. *Am. J. Roentgenol.* **148,** 411–414 (1987).
17. R. E. Wendt, R. Rokey, W. Wong, A. Marks. Magnetic resonance velocity measurements in small arteries. Comparison with Doppler ultrasonic measurements in the aortas of normal rabbits. *Invest. Radiol.* **27,** 499–503 (1992).
18. N. J. Pelc, F. G. Sommer, D. R. Enzmann, L. R. Pelc, G. H. Glover, Accuracy and precision of phase contrast flow measurements. *Radiology* **181(P),** 189 (1991).
19. C. Tang, D. D. Blatter, D. L. Parker, Accuracy of phase-contrast flow measurements in the presence of partial-volume effects. *J. Magn. Reson. Imaging* **3,** 377–385 (1993).
20. R. L. Wolf, R. L. Ehman, S. J. Riederer, P. J. Rossman, Analysis of systematic and random error in MR volumetric flow measurements. *Magn. Reson. Med.* **30,** 82–91 (1993).
21. M. B. M. Hofman, W. van Asten, M. Kouwenhoven, M. Sprenger, MR versus Doppler velocity measurements, caveats in the use of linear array Doppler, *in* "Proc., SMRM, 10th Annual Meeting, 1991," p. 810.
22. C. R. Deane, F. Forsberg, N. Thomas, V. C. Roberts, Accuracy of colour Doppler ultrasound velocity measurements in small vessels. *J. Biomed. Eng.* **13,** 249–254 (1991).
23. C. J. Drost, Homogeneous full flow illumination to ultrasonic systems, *in* "Proc., 31st Annual Conference of Engineering in Medicine and Biology, 1978," p. 183.
24. D. L. Franklin, D. W. Baker, R. M. Ellis, R. F. Rushmer, *IRE Trans. Med. Electron* **ME-6,** 204 (1959).
25. M. A. Portman, S. James, F. W. Heineman, R. S. Balaban, Simultaneous monitoring of coronary blood flow and 31P NMR detected myocardial metabolites. *Magn. Reson. Med.* **7,** 243–247 (1988).
26. G. T. Gullberg, F. W. Wehrli, A. Shimakawa, M. A. Simons, MR vascular imaging with a fast gradient refocusing pulse sequence and reformatted images from transaxial sections. *Radiology* **165,** 241–246 (1987).
27. J. P. Groen, R. G. de Graaf, P. van Dijk, MR angiography based on inflow, *in* "Proc., SMRM, 7th Annual Meeting, 1988," p. 906.
28. D. A. Sebok, D. Wilkerson, W. Schroder, R. Mezrich, M. Zatina, Interleaved magnetic resonance and ultrasound by electronic synchronization. *Invest. Radiol.* **26,** 353–357 (1991).
29. J. M. Bland, D. G. Altman, Statistical methods for assessing agreement between two methods of clinical measurement. *Lancet* **Feb.,** 307–310 (1986).
30. M. Tarnawski, D. A. Porter, M. J. Graves, M. G. Taylor, M. A. Smith, Flow determination in small diameter vessels by magnetic resonance imaging, *in* "Proc., SMRM, 8th Annual Meeting, 1989," p. 896.
31. T. E. Conturo, G. D. Smith, Signal-to-noise in phase angle reconstruction: dynamic range extension using phase reference offsets. *Magn. Reson. Imaging* **15,** 420–437 (1990).
32. D. A. Sebok, D. Wilkerson, R. S. Mezrich, M. Zatina, In-vivo comparison of phase shift MR and ultrasound flow measurements, *in* "Proc., SMRM, 9th Annual Meeting, 1990," p. 467.